



111104 085832

NIST  
PUBLICATIONS

NISTIR 5219

---

---

# THE DISPERSION OF FIRE SUPPRESSION AGENTS DISCHARGED FROM HIGH PRESSURE VESSELS: ESTABLISHING INITIAL/BOUNDARY CONDITIONS FOR THE FLOW OUTSIDE THE VESSEL

---

---

Leonard Y. Cooper

Building and Fire Research Laboratory  
Gaithersburg, Maryland 20899

**NIST**

United States Department of Commerce  
Technology Administration  
National Institute of Standards and Technology

~~QC~~

100

.U56

#5219

1993



**THE DISPERSION OF FIRE SUPPRESSION  
AGENTS DISCHARGED FROM HIGH  
PRESSURE VESSELS: ESTABLISHING  
INITIAL/BOUNDARY CONDITIONS FOR THE  
FLOW OUTSIDE THE VESSEL**

---

---

Leonard Y. Cooper

September 1993  
Building and Fire Research Laboratory  
National Institute of Standards and Technology  
Gaithersburg, MD 20899



**U.S. Department of Commerce**  
Ronald H. Brown, *Secretary*  
**Technology Administration**  
Mary L. Good, *Under Secretary for Technology*  
National Institute of Standards and Technology  
Arati Prabhakar, *Director*

*Sponsored by:*  
U.S. Air Force  
Wright Patterson AFB 45433-6563



# TABLE OF CONTENTS

	<u>Page</u>
TABLE OF CONTENTS .....	iii
LIST OF TABLES .....	iv
LIST OF FIGURES .....	v
ABSTRACT .....	1
BACKGROUND AND PURPOSE .....	2
A MODEL OF THE DISCHARGE PROCESS .....	2
MODELING THE EARLY DEVELOPMENT OF THE JET: FROM THE EXIT SECTION OF THE DISCHARGE VESSEL TO A NEARBY SECTION IN A STATE OF THERMODYNAMIC EQUILIBRIUM AND COMPLETED DROPLET FORMATION .....	3
General Considerations .....	3
The Initial Section of the Jet .....	4
Assumptions of the Phenomena in the Transition Region: From the Nozzle/Orifice to the Initial Section .....	4
The Initial State: A Summary of Assumptions and Approximations and Their Implications .....	5
<i>At the initial section</i> .....	5
<i>Conservation of mass:</i> .....	6
<i>Conservation of energy [and using Eq. (6)]:</i> .....	6
<i>Droplet size</i> .....	7
<i>Initial jet radius</i> .....	7
<i>Parameters defining the initial state</i> .....	7
Completing the Description of the Initial State .....	7
<i>Modeling the liquid agent as incompressible</i> .....	7
<i>Modeling the agent gas as a perfect gas</i> .....	8
<i>The solution for <math>V_{LA}</math> and <math>x_I</math></i> .....	8
ALGORITHM FOR DETERMINING THE INITIAL STATE .....	9
EXAMPLE APPLICATION OF THE ALGORITHM .....	10
Conditions for Example Discharges and Temperature-Dependent Agent Property Functions .....	10
Results of the Example Calculations .....	11
REFERENCES .....	13
NOMENCLATURE .....	14

**APPENDIX: MATERIAL PROPERTY FUNCTIONS FOR FREON 22 ( $\text{CHClF}_2$ ) AND  
HALON 1301 ( $\text{CBrF}_3$ ) ..... 16**

## LIST OF TABLES

	<u>Page</u>	
Table 1.	Geometric parameters, orifice coefficient, and initial conditions for example discharges from a Figure-1-type configuration with no holding tank. . . . .	19
Table 2.	Constant properties of the initial state for the example calculations. . . . .	19
Table 3.	Initial state of a Freon 22 ( $\text{CHClF}_2$ ) jet from Figure-1-type vessel with characteristics of Table 1, constant initial state properties of Table 2, and with $r_I = 10r_{LJ} = 10C_D^{1/2}r_N = 0.07378\text{m}$ . . . . .	20
Table 4.	Initial state of a Halon 1301 ( $\text{CBrF}_3$ ) jet from Figure-1-type vessel with characteristics of Table 1, constant initial state properties of Table 2, and with $r_I = 10r_{LJ} = 10C_D^{1/2}r_N = 0.07378\text{m}$ . . . . .	21
Table 5.	Initial state of a Freon 22 ( $\text{CHClF}_2$ ) jet from Figure-1-type vessel with characteristics of Table 1, constant initial state properties of Table 2, and with $r_I = 20r_{LJ} = 20C_D^{1/2}r_N = 0.1476\text{m}$ . . . . .	22
Table 6.	Initial state of a Halon 1301 ( $\text{CBrF}_3$ ) jet from Figure-1-type vessel with characteristics of Table 1, constant initial state properties of Table 2, and with $r_I = 20r_{LJ} = 20C_D^{1/2}r_N = 0.1476\text{m}$ . . . . .	23

## LIST OF FIGURES

		<u>Page</u>
Figure 1.	The experimental arrangement. ....	24
Figure 2.	Path in the enthalpy - pressure plane of the thermodynamic state of the initially liquid agent as it flows from inside to outside the pressure vessel and achieves a stable two-phase state at the initial section. ....	25
Figure 3.	Sketch of the discharging agent, the transition region, and the initial section, $z = z_I$ . ....	26
Figure 4.	Sketch of the velocity and mass fluxes of agent gas and agent liquid droplets at the initial section, $z = z_I$ . ....	27
Figure 5.	Plot of Table 3 results for $P_{DV}$ as a function of time during vessel discharge of Freon 22. ....	28
Figure 6.	Plot of Table 3 results for $V_{LA}$ as a function of time during vessel discharge of Freon 22. ....	29
Figure 7.	Plots of Table 3 results for $\zeta$ and $x_I$ as functions of time during vessel discharge of Freon 22. ....	30
Figure 8.	Plots of Table 3 results for $dM_{LAL}/dt$ and $dM_{LAG}/dt$ as functions of time during vessel discharge of Freon 22. ....	31

**THE DISPERSION OF FIRE SUPPRESSION AGENTS DISCHARGED FROM HIGH PRESSURE VESSELS: ESTABLISHING INITIAL/BOUNDARY CONDITIONS FOR THE FLOW OUTSIDE THE VESSEL**

**Leonard Y. Cooper  
Fire Modeling Group  
Building and Fire Research Laboratory  
National Institute of Standards and Technology**

**ABSTRACT**

This work reports on part of an effort to study the dispersion and extinguishment effectiveness of Halon and Halon-alternative fire extinguishment agents discharged from N<sub>2</sub>-pressurized vessels. In the systems under consideration, as the agent exits from the vessel, thermodynamic and fluid-dynamic instabilities lead to flashing and break-up of the agent into a two-phase droplet/gaseous jet mixture. This occurs in a transition region relatively close to the vessel exit orifice/nozzle. Downstream of this region the two-phase agent jet then mixes with the ambient air environment and is dispersed in the protected space.

A mathematical model has been developed previously to simulate the time-dependent discharge of the agent from the pressure vessel. Using the output of this model and thermodynamic and fluid-dynamic considerations of the phenomena in the transition section, the present work develops a method for determining a set of initial/boundary conditions at an initial section of the jet, downstream of the transition region. These initial/boundary conditions are in a form that can be used to formulate and solve the problem of the development and dispersal of the ensuing mixed air/two-phase-agent jet.

Example applications of the developed methodology are presented. These are for agent discharge from a half-liter cylindrical discharge vessel with a circular discharge nozzle/orifice of diameter 0.019m. Simulations involve discharge of the vessel when it is half-filled with either Freon 22 or Halon 1301 and then pressurized with N<sub>2</sub> to 41.37x10<sup>5</sup>Pa (600psi).

**Key Words:** agents, aircraft fire safety, discharge, fire extinguishment, fire safety, halon, halon alternatives

## BACKGROUND AND PURPOSE

The Building and Fire Research Laboratory (BFRL) of the National Institute of Standards and Technology (NIST) is carrying out a Program for the US Air Force to study the dispersion and extinguishment effectiveness of Halon and Halon-alternative fire extinguishment agents discharged from N<sub>2</sub>-pressurized vessels. This is being carried out in support of an effort to advance the technology of fire safety in US Air Force aircraft.

One objective of the program is to measure and/or predict the dispersion of a discharging agent throughout a protected space. Time-dependent agent concentrations associated with a particular agent discharge and threat scenario would be used as a basis for estimating extinguishment effectiveness.

This work focuses on one aspect of the problem of predicting agent dispersion by means of mathematical/computer modeling.

The strategy to predict agent dispersion characteristics involves two basic mathematical model components: 1) a model to simulate the time-dependent discharge of the agent from the high-pressure discharge vessel; and 2) a model to simulate the development and dispersal of the ensuing mixed air/two-phase-agent jet.

A critical element in exercising any component-2 model is to establish a set of initial/boundary conditions for the jet. This must be at a location of the jet axis near the exit section of the discharge vessel. The initial/boundary conditions would be derived from the predictions of the component-1 model. The purpose of this work is to develop a method to estimate the initial conditions from the predictions of the component-1 model described in [1].

## A MODEL OF THE DISCHARGE PROCESS

In response to the above-mentioned Program objectives a component-1-type mathematical model of agent discharge was developed in [1]. The model is designed to simulate agent discharge for test or field-deployed system configurations depicted in Figure 1. This involves a cylindrical discharge vessel with a short, circular, exit nozzle/orifice. The vessel is filled with pure agent (part liquid and part gas). The agent is then pressurized with N<sub>2</sub> to some prescribed value. Liquid agent and some dissolved N<sub>2</sub> is in the lower part of the vessel. Above this is a mixture of gaseous agent and N<sub>2</sub>. In the case of a field-deployed system, liquid-agent discharge is initiated by actuation of an explosive cap sealing the exit nozzle/orifice.

A Figure-1 test configuration, which would be used to simulate field-deployed system discharges under laboratory conditions, is equipped with the indicated high-pressure N<sub>2</sub> holding tank. This is connected to the discharge vessel *via* an orifice. This system simulates the field-deployed system by using a rupture diaphragm over the exit nozzle/orifice (nominal rupture pressure same as the pre-discharge pressure of the field-deployed system) rather than an explosive cap. An experimental run begins with the onset of through-orifice N<sub>2</sub> flow from the holding tank. The vessel is pressurized to the point of diaphragm rupture and this is immediately followed by vessel discharge to the atmospheric pressure environment. Note that systems of interest in the present study typically involve initial discharge vessel pressures, P<sub>DV</sub>, of several tens of atmospheres, where, in the "upside down"

Figure-1 configuration and at the time that liquid discharge is being completed,  $P_{DV}$  is still large enough to preclude flashing of the liquid in the vessel.

The reader is referred to Reference [1] for a detailed description of the model and for results of simulations carried out to establish an experimental design and procedure which would be expected to closely simulate field-deployed system discharges.

The model simulates the time-dependent discharge of Figure-1-type systems up to the time that the last of the liquid agent is ejected from the vessel. For a specified set of geometric system parameters, agent material, and initial conditions, key results of a model simulation are the rate of liquid agent discharged from the vessel and the vessel pressure. This work develops a procedure to use these results along with other considerations to estimate initial/boundary conditions for a component-2-type model simulation of the development and dispersal of the ensuing mixed air/two-phase-agent jet.

## MODELING THE EARLY DEVELOPMENT OF THE JET: FROM THE EXIT SECTION OF THE DISCHARGE VESSEL TO A NEARBY SECTION IN A STATE OF THERMODYNAMIC EQUILIBRIUM AND COMPLETED DROPLET FORMATION

### General Considerations

It is assumed that within the discharge vessel and upstream of the exit nozzle/orifice the velocity of the liquid agent is so small that its kinetic energy can be neglected in considerations of its thermodynamic state. Therefore, the thermodynamic state upstream of the nozzle/orifice position can be estimated by the pressure in the discharge vessel,  $P_{DV}$ , and the temperature there of the liquid agent,  $T_{DV,AL}$ . Note that in most applications it is expected that  $T_{DV,AL}$  is well approximated by  $T_{AMB}$ , the ambient temperature outside the vessel. A point representing the state of the liquid agent in the vessel is indicated in the sketched pressure-enthalpy ( $P, h$ ) diagram of Figure 2.

Because of the relatively-short nozzle/orifice design under consideration, the time interval for the liquid to approach it, pass through it, and enter the outside environment is very small. For conditions related to the NIST Program this is of the order of  $10^{-3}$ s. During this time interval the pressure of the traversing liquid is reduced from the high  $P_{DV}$  values inside the vessel, of the order of several tens of atmospheres, to pressures of the order of  $P_{AMB}$ , one atmosphere.

As discharging liquid enters and traverses the region of the nozzle/orifice, it will enter and move along super-heated metastable thermodynamic states. While dependent on its changing thermodynamic state in the vessel, ( $P_{DV}$ ,  $T_{DV,AL}$ ), and on its particular thermodynamic properties, as the agent material penetrates the ambient environment it approaches, and likely achieves the  $P_{AMB}$  pressure while still in its metastable liquid state. Thus, downstream of a *vena contracta* the liquid agent develops into a near-uniform-radius liquid jet,  $r_{LJ}$ , which can be described following traditional incompressible fluid-dynamic considerations. See Figure 3. For the relatively large-vapor-pressure agent materials of interest here, a combination of fluid-dynamic and thermodynamic instabilities will then lead to breakup into small droplets and flashing (i.e., rapid evaporation to a two-phase equilibrium thermodynamic state) of the metastable liquid jet [2].

The metastable liquid is expected to move through thermodynamic states on near-isentropic paths. However, as discussed in [1], for a given agent and initial state conditions, ( $P_{DV}$ ,  $T_{DV,AL}$ ), it is

possible that the pressure along such a path will not reach  $P_{AMB}$  prior to an intersection with the agent's spinoidal curve. Moreover, if such an intersection does occur, then at that instant spontaneous nucleation in the liquid is to be expected [3, 4]. It is conjectured that this would lead to near-explosive breakup and flashing of the jet, all of this being initiated within a jet penetration depth (into the outside environment) of the order of a single nozzle/orifice diameter.

Whatever the thermodynamic-state path of the discharging metastable liquid, it is reasonable to assume that a relatively short distance downstream of the nozzle/orifice a thermodynamic equilibrium state and an end to the droplet-formation phenomenon will be achieved. It is also reasonable to assume that, as the agent flows further downstream, developing as a mixed, two-phase, agent/air jet, thermodynamic equilibrium will be maintained, and droplet collision and agglomeration will not play an important role in jet dynamics.

### **The Initial Section of the Jet**

The position along the jet axis where both approximate thermodynamic equilibrium and completion of droplet formation is first achieved will be denoted here as the *initial* position of the jet. Associated with this position is the plane section normal to the jet axis, called the *initial* section of the jet. Similarly, the thermodynamic state and properties of the jet at the initial position will be denoted as its *initial* state and *initial* properties. The region of the flow between the nozzle/orifice discharge section and the initial section will be referred to as the transition region of the jet.

A detailed description of the initial state and properties of the jet would be extremely complicated. This would include the variation across the initial section of air/gaseous-agent concentrations, temperature, and velocity, and of the size, velocity, and temperature distributions of the liquid agent droplets. Note also that in the present application all of these variables of the initial jet flow field would be time-dependent. In general, an accurate detailed description of the initial state of the jet, whether determined by theoretical or experimental means, is either impractical or beyond the current state of technology.

Although it is not possible to provide a detailed description of the initial state of the jet, it is reasonable to expect that an achievable approximate description, suitable for use in a component-2-type model, would yield good approximations of the dispersing-agent-flow-field problem. It is the purpose of this work to provide such an approximate description.

### **Assumptions of the Phenomena in the Transition Region: From the Nozzle/Orifice to the Initial Section**

The dynamic processes that initiate breakup and flashing of the metastable liquid jet and bring it to its initial state are not completely understood. At one extreme, it is possible that the above-mentioned instabilities lead to violent breakup and flashing of the liquid jet immediately upon leaving the exit nozzle/orifice. Such behavior was observed, for example, in some experiments of [5]. Also, toward the completion of the liquid discharge, this was also observed in recent experiments at NIST [6].

The metastable state can also persist even as the liquid jet penetrates relatively deeply into the ambient environment. For example, Reference [5] describes a liquid water jet of diameter  $D = 7.6(10^{-4})\text{m}$ , initially at  $9.03 \times 10^5 \text{Pa}$  (131psi) and 415K, which penetrated up to 0.0254m, corresponding to  $L/D \approx 32$ , before initiation of violent breakup/flashing. Observed in the recent NIST experiments [6] was a liquid Freon 22 jet,  $D \approx 0.02\text{m}$ , initially at  $41.37 \times 10^5 \text{Pa}$  (600psi) and 294K, which penetrated a distance of approximately 0.3m, corresponding to  $L/D \approx 15$ , before initiation of violent breakup/flashing. In this regard it is of interest to note that in the literature of the discharge of flashing liquids from high pressure vessels there is a degree of conventional wisdom that analyses of the two-phase flow phenomena, based on thermodynamic equilibrium states, tend to yield good results when the nozzle/piping from the inside to the outside of a high pressure discharge vessel is at least 0.1m [7].

The initial section will be some incremental distance downstream of the penetration distance of the metastable liquid jet. The studies of [5] and the recent experiments at NIST [6] suggest that this incremental distance will typically not exceed the order of the penetration distance itself. Whatever the distance, it is assumed here that the total length of the transition region is small enough, compared to the characteristic length of the overall agent dispersal problem of interest, that the processes within the transition region can be treated as quasi-steady.

In the transition region it is assumed that momentum transfer and any net work or heat transfer interactions between the penetrating agent jet and the ambient air environment are negligible. Thus, consistent with the analysis of [8] for steady, two-phase, air/evaporating-liquid jets, it is assumed that the jet at the initial section can be approximated as consisting only of a two-phase mixture of agent, with no entrained air. Finally, in the transition section it is assumed that increases in the energy of the liquid due to mechanical work by surface tension forces to form the initial-section droplets are negligible compared to the energy transfers involved in phase-change processes.

### **The Initial State - A Summary of Assumptions and Approximations and Their Implications**

Regarding an estimate of the initial state, the assumptions of the previous paragraph, some additional approximations and assumptions, and their implications are now summarized.

**At the initial section.** The jet is defined by a characteristic initial radius  $r_I$ . The region  $r \leq r_I$  consists of a pure mixture of saturated-agent vapor and liquid (droplets) in thermodynamic equilibrium at temperature,  $T_I$ , and pressure,  $P_I$ , where

$$P_I = P_{\text{AMB}}; r \leq r_I \quad (1)$$

$$T_I = T_{\text{SAT}} = T_{\text{SAT}}(P_{\text{AMB}}); r \leq r_I \quad (2)$$

and where

$$T_{SAT} = T_{SAT}(P), P \leq P_{CR} \quad (3)$$

is the saturation temperature of the agent, a specified function of pressure  $P$ , where  $P$  can not exceed the critical pressure,  $P_{CR}$ . The liquid-agent component of the jet consists of droplets of uniform-radius  $r_{I,D}$  and these are uniformly dispersed over the region  $r \leq r_I$ . The agent droplets and gas have the same uniform axial jet velocity,  $V_{I,A}$ .

$$V_I = V_{I,A}; r \leq r_I \quad (4)$$

where  $V_I = V_I(r)$  is the velocity distribution of the jet at the initial section. There is no agent in  $r > r_I$ .

The region  $r > r_I$  consists of a uniform ambient-temperature/pressure environment ( $P_{AMB}$ ,  $T_{AMB}$ ) of quiescent air.

$$P_I = P_{AMB}; T_I = T_{AMB}; V_{I,AIR} = 0; r > r_I \quad (5)$$

There is no air in  $r \leq r_I$ .

### Conservation of mass:

$$\pi r_I^2 V_{I,A} \rho_{I,A} = dM_{DV,AL}/dt \quad (6)$$

$$\rho_{I,A} = 1/[x_I/\rho_{I,AG} + (1 - x_I)/\rho_{I,AL}] \quad (7)$$

where  $\rho_{I,A}$ ,  $\rho_{I,AL}$  and  $\rho_{I,AG}$  are the average density of the agent, the density of the liquid agent (droplets), and the density of the agent gas at the initial section, respectively;  $x_I$  is the quality of the two-phase flow at the initial section, i.e., the fraction of a mass of agent which is saturated gas;  $M_{DV,AL}$  is the instantaneous mass of liquid agent in the discharge vessel; and the right side of Eq. (6), determined previously from, e.g., the discharge model of [1], is assumed to be specified.

### Conservation of energy [and using Eq. (6)]:

$$h_{DV,AL} = h_{I,AL} + x_I h_{ALG}(T_{SAT}) + V_{I,A}^2/2 \quad (8)$$

$$h_{ALG}(T_{SAT}) = h_{I,AG} - h_{I,AL} \quad (9)$$

where  $h_{DV,AL}$  and  $h_{I,AL}$  are the specific enthalpy of the agent liquid in the discharge vessel and at the initial section, respectively;  $h_{I,AG}$  is the specific enthalpy of the agent gas at the initial section; and  $h_{ALG}$  is the heat of vaporization of the agent at the temperature  $T_{SAT}$ . In Eq. (9),

$$h_{ALG} = h_{ALG}(T), T \leq T_{CR} \quad (10)$$

is a specified function of temperature,  $T$ , where  $T$  can not exceed the critical temperature,  $T_{CR}$ .

A point representing the state of the agent at the initial section is presented in the  $(P, h)$  diagram of Figure 2. Consistent with Eq. (8), this reflects the fact that some of the original enthalpy of the material in its high pressure "rest" state was exchanged for its now-significant kinetic energy.

The sketch of the transition region and of the initial properties as presented in Figure 3 is consistent with the all the above assumptions/approximations.

**Droplet size.** It is assumed that  $r_{LD}$  is specified. Based on [5] it is expected that this will be in the range  $10\mu\text{m} - 100\mu\text{m}$ . Photographic data during future NIST experiments should provide sharper estimates of this parameter. Also, the sensitivity of the downstream agent concentrations to variations of this parameter should be evaluated with component-2 model simulations.

**Initial jet radius.** It is assumed that  $r_I$  is specified. Based on photographic data in [5] and on photographic data already acquired during NIST experiments,  $r_I/r_{LJ}$  seems to be of the order of 10 - 20. Thus, in (what is reasonable to construe visually in high speed photographs as) a region of breakup and flashing of the liquid jet to an initial equilibrium state, the radius of the jet increases by a factor of 10 - 20. Again, the sensitivity of the downstream agent concentrations to variations of this ratio should be evaluated with component-2 model simulations. One would hope that such sensitivity is not great.

**Parameters defining the initial state.** Consistent with the above, the specified parameters of the initial state are  $P_I$ , according to Eq. (1),  $r_{LD}$ , and  $r_I/r_{LJ}$ . Also, for a particular agent of interest,  $T_I$  is specified by (2) and (3). Required to complete the description of the initial state are  $\rho_{I,AL}$ ,  $V_{I,A}$ , and  $x_I$ .

### Completing the Description of the Initial State

**Modeling the liquid agent as incompressible.** For problems of interest here, agent liquid temperatures are expected to be small enough compared to  $T_{CR}$  and vary in a small enough range to permit accurate modeling of the liquid as being incompressible, with density  $\rho_{AL}$ , and as having a constant specific heat,  $C_{AL}$ . Thus,

$$\rho_{I,AL} = \rho_{AL} \quad (11)$$

The values of  $\rho_{AL}$  and  $C_{AL}$  will be taken as

$$\rho_{AL} = \rho_{AL}(T_{AL}); C_{AL} = C_{AL}(T_{AL}); T_{AL} = (T_{SAT} + T_{DV,AL})/2 \quad (12)$$

where  $T_{AL}$  is taken to be the average temperature of the liquid in the discharge vessel and at the initial state, and where  $\rho_{AL}(T)$  and  $C_{AL}(T)$  are specified functions of  $T$

From the assumption of incompressibility it follows that

$$h_{DV,AL} - h_{I,AL} = C_{AL}(T_{DV,AL} - T_{SAT}) + (P_{DV} - P_{AMB})/\rho_{AL} \quad (13)$$

**Modeling the agent gas as a perfect gas.** The agent gas is modeled as a perfect gas.

$$\rho_{I,AG} = P_I/(R_{AG}T_I) = P_{AMB}/(R_{AG}T_{SAT}) \quad (14)$$

where  $R_{AG}$  is the gas constant.

**The solution for  $V_{I,A}$  and  $x_I$ .** As discussed above, it is expected that in most instances the liquid jet will achieve  $P_{AMB}$  prior to its breakup/flashing. Then, Bernoulli's equation leads to

$$dM_{DV,AL}/dt = \pi r_{LJ}^2 \rho_{AL} [2(P_{DV} - P_{AMB})/\rho_{AL}]^{1/2} \quad (15)$$

where  $r_{LJ}$  is determined from the radius of the exit nozzle/orifice,  $r_N$ , and its orifice discharge coefficient,  $C_D$ .

$$(r_{LJ}/r_N)^2 = C_D \quad (16)$$

Substituting Eqs. (9) and (13) into Eq. (8) lead to

$$V_{I,A}^2/2 = C_{AL}(T_{DV,AL} - T_{SAT}) + (P_{DV} - P_{AMB})/\rho_{AL} - x_I h_{ALG}(T_{SAT}) \quad (17)$$

Substituting Eqs. (7) and (15) into Eq. (6) leads to

$$V_{I,A}^2/2 = (r_{LJ}/r_I)^4 [(P_{DV} - P_{AMB})/\rho_{AL}] [(x_I/\varepsilon)(1 - \varepsilon)]^2 \quad (18)$$

$$\varepsilon = \rho_{I,AG}/\rho_{AL} \quad (19)$$

Comparing Eqs. (18) and (17) leads to

$$X^2 + \lambda_2 X - (\lambda_1 + 1) = 0 \quad (20)$$

where

$$X = (x_I/\varepsilon)(1 - \varepsilon)(r_{LJ}/r_I)^2; \quad x_I = X\varepsilon/[(1 - \varepsilon)(r_{LJ}/r_I)^2] \quad (21)$$

$$\lambda_1 = \rho_{AL} C_{AL} (T_{DV,AL} - T_{SAT}) / (P_{DV} - P_{AMB}) \quad (22)$$

$$\lambda_2 = [\varepsilon/(1 - \varepsilon)] \rho_{AL} h_{ALG}(T_{SAT}) / [(P_{DV} - P_{AMB})(r_{LJ}/r_I)^2] \quad (23)$$

The solution to Eq. (20) is

$$X = -(\lambda_2/2) + [(\lambda_2/2)^2 + \lambda_1 + 1]^{1/2} \quad (24)$$

With Eq. (21) and other previous definitions, Eq. (24) provides the solution for  $x_I$ . This would be used, in turn, to obtain  $V_{I,A}$  from Eqs. (17) or (18), thereby completing the description of the initial state.

$$V_{I,A} = 2X[(P_{DV} - P_{AMB})/\rho_{AL}]^{1/2} \quad (17')$$

A sketch of the velocity distribution and the mass flux distributions of gaseous and liquid agent at the initial section are presented in Figure 4.

#### ALGORITHM FOR DETERMINING THE INITIAL STATE

The above solution can be implemented with the following algorithm:

1. Specify agent and its thermodynamic properties, including  $T_{SAT}(P)$  and  $h_{ALG}(T)$ , according to Eqs. (3) and (10), respectively, and  $\rho_{AL}(T)$ ,  $C_{AL}(T)$ .
2. Specify  $r_I/r_{LJ}$  (expected range 10 - 20).
3. Specify  $P_{AMB}$ ,  $T_{AMB}$ , and  $T_{DV,AL}$ . (In most cases expect to specify  $T_{DV,AL} = T_{AMB}$ .)
4. Specify  $T_I = T_{AMB}$  for  $r > r_I$ . Compute  $T_{SAT}(P_{AMB})$  from Eq. (3) and then specify  $T_I = T_{SAT}$  for  $0 \leq r \leq r_I$ .
5. Compute  $h_{ALG}(T_{SAT})$  from Eq. (10).
6. Compute  $T_{AL}$  according to Eq. (12) and then  $\rho_{AL}$  and  $C_{AL}$  according to Eq. (12) and  $\rho_{AL}(T)$  and  $C_{AL}(T)$ , respectively.
7. Compute  $\rho_{I,AG}$  according to Eq. (14) and then  $\varepsilon$  according to Eq. (19).
8. Use a component-1 model, e.g., that of [1], to find the time-dependent values of  $P_{DV}$  for a particular Figure-1-configuration of interest.
9. For a particular value of  $P_{DV}$  compute  $\lambda_1$  and  $\lambda_2$  from Eqs. (22) and (23), and then  $X$  from Eq. (24).
10. Find  $x_I$  from Eq. (21) and  $V_{I,A}$  from Eq. (17').

## EXAMPLE APPLICATION OF THE ALGORITHM

### Conditions for Example Discharges and Temperature-Dependent Agent Property Functions

The algorithm was applied in four example discharge simulations. These involve the agents Freon 22 ( $CHClF_2$ ) and Halon 1301 ( $CBrF_3$ ) and two different  $r_I$  values corresponding to  $r_I = 10r_{LJ}$  and  $20r_{LJ}$ . The examples consider time-dependent agent discharges from a Figure-1 configuration with no holding tank. The geometric parameters, orifice coefficient, and initial conditions assumed in the simulated example discharge calculations are presented in Table 1. These are the same parameters used in the example calculations of [1]. During the discharge, the time-dependent value of  $P_{DV}$  was computed using the component-1-type model of [1].

The material property functions for Freon 22 ( $CHClF_2$ ) and Halon 1301 ( $CBrF_3$ ) which were used in the example calculations are from [9]. These are of the form

$$\text{Molecular weight, } M: M \text{ kg of agent} = 1 \text{ kg-mole of agent} \quad (25)$$

$$P(T_{SAT})/\text{Pa} = \exp[A + B/(T_{SAT}/R) + C \ln(T_{SAT}/R) + D(T_{SAT}/R)^2]; T_1 \leq T_{SAT} \leq T_2 \quad (26)$$

$$\begin{aligned}
h_{\text{ALG}}(T_{\text{SAT}})/[\text{J}/(\text{kg}\cdot\text{mole}\cdot\text{K})] &= Mh_{\text{ALG}}(T_{\text{SAT}})/[\text{J}/(\text{kg}\cdot\text{K})] \\
&= A(1 - T_{\text{SAT}}/T_{\text{CR}})^B; \quad T_1 \leq T_{\text{SAT}} \leq T_2
\end{aligned} \tag{27}$$

$$\begin{aligned}
\rho_{\text{AL}}(T)/(\text{kg}\cdot\text{mole}/\text{m}^3) &= (1/M)\rho_{\text{AL}}(T)/(\text{kg}/\text{m}^3) \\
&= A/B^F; \quad F = \{1 + [1 - (T/R)/C]^D\}; \quad T_1 \leq T \leq T_2
\end{aligned} \tag{28}$$

$$\begin{aligned}
C_{\text{AL}}(T)/[\text{J}/(\text{kg}\cdot\text{mole}\cdot\text{K})] &= MC_{\text{AL}}(T)/[\text{J}/(\text{kg}\cdot\text{K})] \\
&= A + B(T/R) + C(T/R)^2 + D(T/R)^3; \quad T_1 \leq T \leq T_2
\end{aligned} \tag{29}$$

Complete descriptions of these functions for the two agents are presented in the APPENDIX.

$T_{\text{SAT}}$  was obtained as the root of Eq. (26) where, according to Eq. (2) or item 4 of the algorithm, the left hand side was specified as  $P_{\text{AMB}}$ . Then  $T_{\text{AL}}$  was calculated using Eq. (12). Finally,  $h_{\text{ALG}}(T_{\text{SAT}})$ ,  $\rho_{\text{AL}}(T_{\text{AL}})$ , and  $C_{\text{AL}}(T_{\text{AL}})$  were calculated from Eqs. (27), (28), and (29), respectively. The results are presented in Table 2.

### Results of the Example Calculations

The results of the example calculations are tabulated in Table 3 (Freon 22,  $r_1 = 10r_{\text{LJ}} = 10C_{\text{D}}^{1/2}r_{\text{N}} = 0.07378\text{m}$ ), Table 4 (Halon 1301,  $r_1 = 10r_{\text{LJ}} = 10C_{\text{D}}^{1/2}r_{\text{N}} = 0.07378\text{m}$ ), Table 5 (Freon 22,  $r_1 = 20r_{\text{LJ}} = 20C_{\text{D}}^{1/2}r_{\text{N}} = 0.1476\text{m}$ ), and Table 6 (Halon 1301,  $r_1 = 20r_{\text{LJ}} = 20C_{\text{D}}^{1/2}r_{\text{N}} = 0.1476\text{m}$ ). Included in the tables are computed values of the variable  $\zeta$ , which is the dimensionless mass of liquid agent,  $M_{\text{DV,AL}}$ , or dimensionless elevation of the liquid agent in the discharge vessel,  $Z$ .

$$\zeta = M_{\text{DV,AL}}/M_{\text{DV,AL}}(t = 0) = Z/Z(t = 0) \tag{30}$$

The tabulated results of Table 3 for the discharge of Freon 22 ( $r_1 = 10r_{\text{LJ}} = 0.07378\text{m}$ ) are plotted in Figures 5 - 8. These include plots of the time-dependent values of  $P_{\text{DV}}$  (Figure 5),  $V_{\text{I,A}}$  (Figure 6),  $\zeta$  and  $x_1$  (Figure 7), and  $dM_{\text{I,AL}}/dt$  and  $dM_{\text{I,AG}}/dt$  (Figure 8).

A study of the results leads to the following observations:

1. For both Freon 22 and Halon 1301, the times to complete the discharge of liquid agent from the pressure vessel are almost identical at  $0.024 \pm 0.001\text{s}$  (Tables 3 - 6).
2. At the initial section, the quality of the two-phase agent flow,  $x_1$ , is significantly different for the two agents considered, but for a given agent  $x_1$  is relatively independent of  $t$  and  $r_1$ , for the two initial-section radii values considered ( $r_1 = 0.07378\text{m}$  and  $0.1476\text{m}$ ). Thus, for the

cases considered,  $x_I = 0.31 \pm 0.01$  for Freon 22 (Tables 3 and 5) and  $x_I = 0.54 \pm 0.02$  for Halon 1301 (Tables 4 and 6).

3. At the initial section, for a given agent, and for the two initial-section radii values considered, the mass flow rates of liquid or gaseous agent are almost identical at any particular time during the discharge. [For example: for Freon 22, approximately half-way through the discharge at  $t = 0.01252s$ , values of  $dM_{I,AL}/dt$  for  $r_I = 0.07378m$  and  $r_I = 0.1476m$  are  $8.59kg/s$  (Table 3) and  $8.49kg/s$  (Table 5), respectively; and for Halon 1301, approximately half-way through the discharge at  $t = 0.01222s$ , values for  $dM_{I,AL}/dt$  for  $r_I = 0.07378m$  and  $r_I = 0.1476m$  are  $6.95kg/s$  (Table 4) and  $8.59kg/s$  (Table 6), respectively.] However, over the course of the discharge, these mass flow rates are reduced to approximately two thirds of their initial value. [For example: for Freon 22 and  $r_I = 0.07378$ , the values of  $dM_{I,AL}/dt$  at  $t = 0$  and  $t = 0.2326s$  (near the end of the liquid discharge) are  $11.78kg/s$  and  $7.34kg/s$ , respectively (Table 3 and Figure 5); and for Halon 1301, and  $r_I = 0.07378$ , the values of  $dM_{I,AL}/dt$  at  $t = 0$  and  $t = 0.2443s$  (near the end of the liquid discharge) are  $9.26kg/s$  and  $5.88kg/s$ , respectively (Table 4).]

## REFERENCES

- [1] Cooper, L.Y., Discharge of Fire Suppression Agents From a Pressurized Vessel: Mathematical Model and Its Application to Experimental Design, to appear as NISTIR, National Institute of Standards and Technology, 1993.
- [2] Leinhard, J.H. and Day, James B., The Breakup of Superheated Liquid Jets, *Journal of Basic Engineering*
- [3] Reid, R.C., Superheated Liquids - A Laboratory Curiosity and, Possibly, an Industrial Curse, *Chemical Engineering Education*, pp. 60-87, Spring 1978.
- [4] Modell, M. and Reid, R.C., Thermodynamics and Its Applications, Prentice Hall, 2nd Edition, 1983.
- [5] Brown, R. and York, J.L., Spray Formed by Flashing Liquid Jets, *AIChE Journal*, Vol. 8, No. 2, pp. 149-153, May 1962.
- [6] Yang, J.C., private communication, National Institute of Standards and Technology, Gaithersburg MD, 1992.
- [7] Leung, J.C. and Nazario, F.N., Two-Phase Flashing Flow Methods and Comparisons, *Journal Loss Prevention Process Industry*, Vol. 3, pp. 253-260, April 1990.
- [8] Epstein, M. *et al*, One-Dimensional Modeling of Two-Phase Jet Expansion and Impingement, Thermal-Hydraulics of Nuclear Reactors, Vol. II, 2nd International Topical Meeting on Nuclear Reactor Thermal Hydraulics, Santa Barbara California Jan. 11-14, 1983.
- [9] Daubert, T.E. and Danner, R.P., *Physical and Thermodynamic Properties of Pure Chemicals*, Hemisphere, 1992.

## NOMENCLATURE

A,B,C,D	constants, Eqs. (A2) - (A5)
$C_{AL}$	constant specific heat of liquid agent
$C_D$	orifice coefficient
D	diameter of a liquid jet
F	Eqs. (28) and (A4)
h	specific enthalpy
$h_{ALG}$	specific heat of vaporization of the agent
$h_{DV,AL}$	h of agent liquid in the discharge vessel
$h_{I,AG}$ ( $h_{I,AL}$ )	h of agent gas (liquid) at the initial section
L	length of liquid jet
M	molecular weight
$dM_{I,AG}/dt$ ( $dM_{I,AL}/dt$ )	mass flow rate of agent gas (liquid) at the initial section
$M_{DV,AL}$	mass of liquid agent in the discharge vessel
P	pressure
$P_{AMB}$	p of the ambient environment
$P_{CR}$	critical pressure
$P_{DV}$	p in the discharge vessel
$P_I$	p at the initial section
$R_{AG}$	gas constant for the agent gas
r	radius
$r_I$	r of two-phase agent jet at the initial section
$r_{I,D}$	r of agent droplets at initial section
$r_L$	r of the liquid jet outside the discharge vessel

$r_N$	r of the discharge vessel's exit nozzle/orifice
$T$	absolute temperature
$T_{AL}$	T of liquid agent
$T_{AMB}$	T of ambient environment
$T_{DV,AL}$	T of liquid agent in the discharge vessel
$T_I$	T at the initial section
$T_{SAT}$	saturation temperature of the agent
$T_1, T_2$	constant temperatures, Eqs. (A2) - (A5)
$t$	time
$t_{BURST}$	t when the diaphragm bursts
$V_I$	velocity at the initial section
$V_{I,A}$	$V_I$ of agent
$V_{I,AIR}$	$V_I$ of air
$X$	Eq. (21)
$x_I$	quality of the two-phase agent flow at the initial section
$Z$	distance of the liquid/gas agent interface above the exit nozzle/orifice
$z$	distance along the jet axis from the exit orifice/nozzle
$z_I$	z at the initial section
$\varepsilon$	Eq. (19)
$\lambda_1, \lambda_2$	Eqs. (21) and (22)
$\rho_{LA}$	average density of the agent jet at the initial section
$\rho_{I,AG} (\rho_{I,AL})$	density of the agent liquid (gas) at the initial section
$\rho_{AL}$	density of liquid agent
$\zeta$	dimensionless elevation of the liquid/gas interface, Eq. (30)

**APPENDIX: MATERIAL PROPERTY FUNCTIONS FOR FREON 22 (CHClF<sub>2</sub>) AND HALON 1301 (CBrF<sub>3</sub>)**

The following material property functions for Freon 22 (CHClF<sub>2</sub>) and Halon 1301 (CBrF<sub>3</sub>) were used in the example calculations [9]:

$$\text{Molecular weight} = M \text{ kg of agent} = \text{kg-mole of agent} \quad (\text{A1})$$

		<u>Freon 22 (CHClF<sub>2</sub>)</u>		<u>Halon 1301 (CBrF<sub>3</sub>)</u>
M	=	86.468		148.910

$$P(T_{\text{SAT}})/\text{Pa} = \exp[A + B/(T_{\text{SAT}}/R) + C \ln(T_{\text{SAT}}/R) + D(T_{\text{SAT}}/R)^2]; \quad T_1 \leq T_{\text{SAT}} \leq T_2 \quad (\text{A2})$$

		<u>Freon 22 (CHClF<sub>2</sub>)</u>		<u>Halon 1301 (CBrF<sub>3</sub>)</u>
A	=	9.7882(10)		6.2780(10)
B	=	- 4.7735(10 <sup>-3</sup> )		- 3.3770(10 <sup>-3</sup> )
C	=	- 1.2317(10)		- 6.7461
D	=	2.4173(10 <sup>-5</sup> )		1.4407(10 <sup>-5</sup> )
T <sub>1</sub>	=	115.73K		105.15K
T <sub>2</sub>	=	369.30K		340.15K

$$\begin{aligned}
h_{\text{ALG}}(T_{\text{SAT}})/(\text{J/kg-mole}) &= Mh_{\text{ALG}}(T_{\text{SAT}})/(\text{J/kg}) \\
&= A(1 - T_{\text{SAT}}/T_{\text{CR}})^B; \quad T_1 \leq T_{\text{SAT}} \leq T_2
\end{aligned}
\tag{A3}$$

		<u>Freon 22 (CHClF<sub>2</sub>)</u>	<u>Halon 1301 (CBrF<sub>3</sub>)</u>
A	=	2.9617(10 <sup>7</sup> )	2.5070(10 <sup>7</sup> )
B	=	3.8600(10 <sup>-1</sup> )	3.5700(10 <sup>-1</sup> )
T <sub>CR</sub>	=	369.30K	340.15K
T <sub>1</sub>	=	115.73K	105.15K
T <sub>2</sub>	=	369.30K	340.15K

$$\begin{aligned}
\rho_{\text{AL}}(T)/(\text{kg-mole/m}^3) &= \rho_{\text{AL}}(T)/(\text{Mkg/m}^3) \\
&= A/B^F; \quad F = \{1 + [1 - (T/R)/C]^D\}; \quad T_1 \leq T \leq T_2
\end{aligned}
\tag{A4}$$

		<u>Freon 22 (CHClF<sub>2</sub>)</u>	<u>Halon 1301 (CBrF<sub>3</sub>)</u>
A	=	1.5956	1.3435
B	=	2.6605(10 <sup>-1</sup> )	2.6995(10 <sup>-1</sup> )
C	=	3.6930(10 <sup>2</sup> )	3.4015(10 <sup>2</sup> )
D	=	2.8123(10 <sup>-1</sup> )	2.8006(10 <sup>-1</sup> )
T <sub>1</sub>	=	115.73K	105.15K
T <sub>2</sub>	=	369.30K	340.15K

$$C_{AL}(T)/[J/(kg\text{-mole}\cdot K)] = MC_{AL}(T)/[J/(kg\cdot K)] \quad (A5)$$

$$= A + B(T/R) + C(T/R)^2 + D(T/R)^3; \quad T_1 \leq T \leq T_2$$

		<u>Freon 22 (CHClF<sub>2</sub>)</u>	<u>Halon 1301 (CBrF<sub>3</sub>)</u>
A	=	9.4660(10 <sup>4</sup> )	1.1421(10 <sup>5</sup> )
B	=	3.9300(10 <sup>1</sup> )	- 1.3150(10 <sup>2</sup> )
C	=	- 8.1740(10 <sup>-1</sup> )	6.1200(10 <sup>-1</sup> )
D	=	2.7910(10 <sup>-3</sup> )	0
T <sub>1</sub>	=	115.73K	193.15K
T <sub>2</sub>	=	369.30K	298.15K

**Table 1. Geometric parameters, orifice coefficient, and initial conditions for example discharges from a Figure-1-type configuration with no holding tank.**

Length of discharge vessel = $Z_{DV}$ =	0.2546m
Cross-section area of discharge vessel = $A_{DV}$ =	$0.1963 \times 10^{-2} \text{m}^2$
Volume of discharge vessel = $V_{DV}$ =	$0.500 \times 10^{-3} \text{m}^3$
Area of exit nozzle/orifice = $A_O$ =	$0.2850 \times 10^{-3} \text{m}^2$
Radius of exit nozzle/orifice = $r_O$ =	$0.9525 \times 10^{-2} \text{m}$
Discharge coefficient of exit nozzle/orifice = $C_D$ =	0.6
Initial volume of agent liquid in discharge vessel = $M_{DV,AL,1}$ =	$0.250 \times 10^{-3} \text{m}^3$
Initial temperature of gas in the discharge vessel = $T_{DV,1}$ =	294K
Initial pressure in discharge vessel = $P_{DV,1}$ =	$41.36 \times 10^5 \text{Pa}$ (600psi)
Temperature of agent liquid in discharge vessel = $T_{DV,AL}$ =	294K

**Table 2. Constant properties of the initial state for the example calculations.**

	<u>Freon 22 (CHClF<sub>2</sub>)</u>	<u>Halon 1301 (CBrF<sub>3</sub>)</u>
$T_{SAT}$	232K	215K
$T_{AL}$	263K	254.5K
$h_{ALG}(T_{SAT})$	$0.234 \times 10^6 \text{J/kg}$	$0.118 \times 10^6 \text{J/kg}$
$\rho_{AL}(T_{AL})$	$0.132 \times 10^4 \text{kg/m}^3$	$0.180 \times 10^4 \text{kg/m}^3$
$C_{AL}(T_{AL})$	$0.115 \times 10^4 \text{J/(kg} \cdot \text{K)}$	$0.809 \times 10^3 \text{J/(kg} \cdot \text{K)}$

Table 3. Initial state of a Freon 22 ( $\text{CHClF}_2$ ) jet from Figure-1-type vessel with characteristics of Table 1, constant initial state properties of Table 2, and with  $r_I = 10r_{LJ} = 10C_D^{1/2}r_N = 0.07378\text{m}$ .

$$\rho_{AL} = 1320\text{kg/m}^3$$

$$\rho_{I,AG} = 3.58\text{kg/m}^3$$

$$T_{I,A} = 232\text{K}$$

t	$P_{DV}$	$\zeta$	$V_{I,A}$	$x_I$	$dM_{I,AG}/dt$	$dM_{I,AL}/dt$
[s]	[Pa]		[m/s]		[kg/s]	[kg/s]
0	0.4135E+07	1.0000	122.73	0.3022	5.10	11.78
0.00179	0.3663E+07	0.9031	115.46	0.3025	4.80	11.07
0.00358	0.3299E+07	0.8117	109.49	0.3028	4.55	10.48
0.00537	0.3008E+07	0.7248	104.46	0.3030	4.34	9.99
0.00716	0.2769E+07	0.6417	100.14	0.3032	4.16	9.57
0.00895	0.2570E+07	0.5620	96.37	0.3033	4.01	9.20
0.01073	0.2401E+07	0.4851	93.05	0.3034	3.87	8.88
0.01252	0.2255E+07	0.4108	90.08	0.3035	3.75	8.59
0.01431	0.2128E+07	0.3389	87.41	0.3036	3.63	8.33
0.01610	0.2016E+07	0.2690	84.99	0.3037	3.53	8.10
0.01789	0.1917E+07	0.2010	82.78	0.3038	3.44	7.89
0.01968	0.1829E+07	0.1347	80.76	0.3039	3.36	7.69
0.02147	0.1749E+07	0.0701	78.88	0.3039	3.28	7.51
0.02326	0.1677E+07	0.0069	77.15	0.3040	3.21	7.34

Table 4. Initial state of a Halon 1301 (CBrF<sub>3</sub>) jet from Figure-1-type vessel with characteristics of Table 1, constant initial state properties of Table 2, and with  $r_I = 10r_{LJ} = 10C_D^{1/2}r_N = 0.07378\text{m}$ .

$$\rho_{AL} = 1800\text{kg/m}^3$$

$$\rho_{LAG} = 6.17\text{kg/m}^3$$

$$T_{I,A} = 215\text{K}$$

t	P <sub>DV</sub>	ζ	V <sub>LA</sub>	x <sub>I</sub>	dM <sub>I,AG</sub> /dt	dM <sub>I,AL</sub> /dt
[s]	[Pa]		[m/s]		[kg/s]	[kg/s]
0	0.4135E+07	1.0000	142.83	0.5181	9.95	9.26
0.00204	0.3687E+07	0.9030	135.28	0.5205	9.43	8.69
0.00407	0.3338E+07	0.8111	128.99	0.5224	8.99	8.22
0.00611	0.3057E+07	0.7236	123.64	0.5239	8.62	7.83
0.00814	0.2826E+07	0.6397	118.99	0.5252	8.29	7.50
0.01018	0.2631E+07	0.5590	114.91	0.5263	8.01	7.21
0.01222	0.2465E+07	0.4812	111.28	0.5273	7.76	6.95
0.01425	0.2322E+07	0.4058	108.03	0.5281	7.53	6.73
0.01629	0.2197E+07	0.3327	105.08	0.5289	7.32	6.52
0.01832	0.2086E+07	0.2616	102.40	0.5295	7.14	6.34
0.02036	0.1988E+07	0.1924	99.94	0.5301	7.97	6.17
0.02240	0.1899E+07	0.1248	97.67	0.5307	6.81	6.02
0.02443	0.1820E+07	0.0588	95.58	0.5311	6.66	5.88

Table 5. Initial state of a Freon 22 (CHClF<sub>2</sub>) jet from Figure-1-type vessel with characteristics of Table 1, constant initial state properties of Table 2, and with  $r_I = 20r_{LJ} = 20C_D^{1/2}r_N = 0.1476m$ .

$$\rho_{AL} = 1320\text{kg/m}^3$$

$$\rho_{I,AG} = 3.58\text{kg/m}^3$$

$$T_{I,A} = 232\text{K}$$

t	P <sub>DV</sub>	ζ	V <sub>I,A</sub>	x <sub>I</sub>	dM <sub>I,AG</sub> /dt	dM <sub>I,AL</sub> /dt
[s]	[Pa]		[m/s]		[kg/s]	[kg/s]
0.00000	0.4135E+07	1.0000	32.21	0.3172	5.36	11.53
0.00179	0.3663E+07	0.9030	30.13	0.3158	5.01	10.86
0.00358	0.3299E+07	0.8117	28.45	0.3148	4.73	10.30
0.00537	0.3008E+07	0.7248	27.05	0.3139	4.50	9.83
0.00716	0.2769E+07	0.6417	25.86	0.3132	4.30	9.43
0.00895	0.2570E+07	0.5620	24.83	0.3126	4.13	9.08
0.01073	0.2401E+07	0.4851	23.92	0.3121	3.98	8.77
0.01252	0.2255E+07	0.4108	23.12	0.3117	3.85	8.49
0.01431	0.2128E+07	0.3389	22.40	0.3113	3.73	8.24
0.01610	0.2016E+07	0.2690	21.75	0.3109	3.62	8.02
0.01789	0.1917E+07	0.2010	21.16	0.3107	3.52	7.81
0.01968	0.1829E+07	0.1347	20.62	0.3104	3.43	7.62
0.02147	0.1749E+07	0.0701	20.12	0.3102	3.35	7.44
0.02326	0.1677E+07	0.0069	19.67	0.3099	3.27	7.28

Table 6. Initial state of a Halon 1301 (CBrF<sub>3</sub>) jet from Figure-1-type vessel with characteristics of Table 1, constant initial state properties of Table 2, and with  $r_1 = 20r_{LJ} = 20C_D^{1/2}r_N = 0.1476\text{m}$ .

$$\rho_{AL} = 1800\text{kg/m}^3$$

$$\rho_{I,AG} = 6.17\text{kg/m}^3$$

$$T_{I,A} = 215\text{K}$$

t	P <sub>DV</sub>	ζ	V <sub>I,A</sub>	x <sub>I</sub>	dM <sub>I,AG</sub> /dt	dM <sub>I,AL</sub> /dt
[s]	[Pa]		[m/s]		[kg/s]	[kg/s]
0.00000	0.4135E+07	1.0000	38.48	0.5583	10.73	8.49
0.00204	0.3687E+07	0.9030	36.17	0.5566	10.08	8.03
0.00407	0.3338E+07	0.8111	34.28	0.5552	9.56	7.66
0.00611	0.3057E+07	0.7236	32.69	0.5541	9.11	7.33
0.00814	0.2826E+07	0.6397	31.33	0.5532	8.73	7.05
0.01018	0.2631E+07	0.5590	30.15	0.5524	8.41	6.81
0.01222	0.2465E+07	0.4812	29.11	0.5518	8.12	6.59
0.01425	0.2322E+07	0.4058	28.19	0.5512	7.86	6.40
0.01629	0.2197E+07	0.3327	27.36	0.5507	7.63	6.22
0.01832	0.2086E+07	0.2616	26.60	0.5503	7.42	6.06
0.02036	0.1988E+07	0.1924	25.92	0.5499	7.23	5.91
0.02240	0.1899E+07	0.1248	25.29	0.5496	7.05	5.78
0.02443	0.1820E+07	0.0588	24.71	0.5492	6.89	5.65

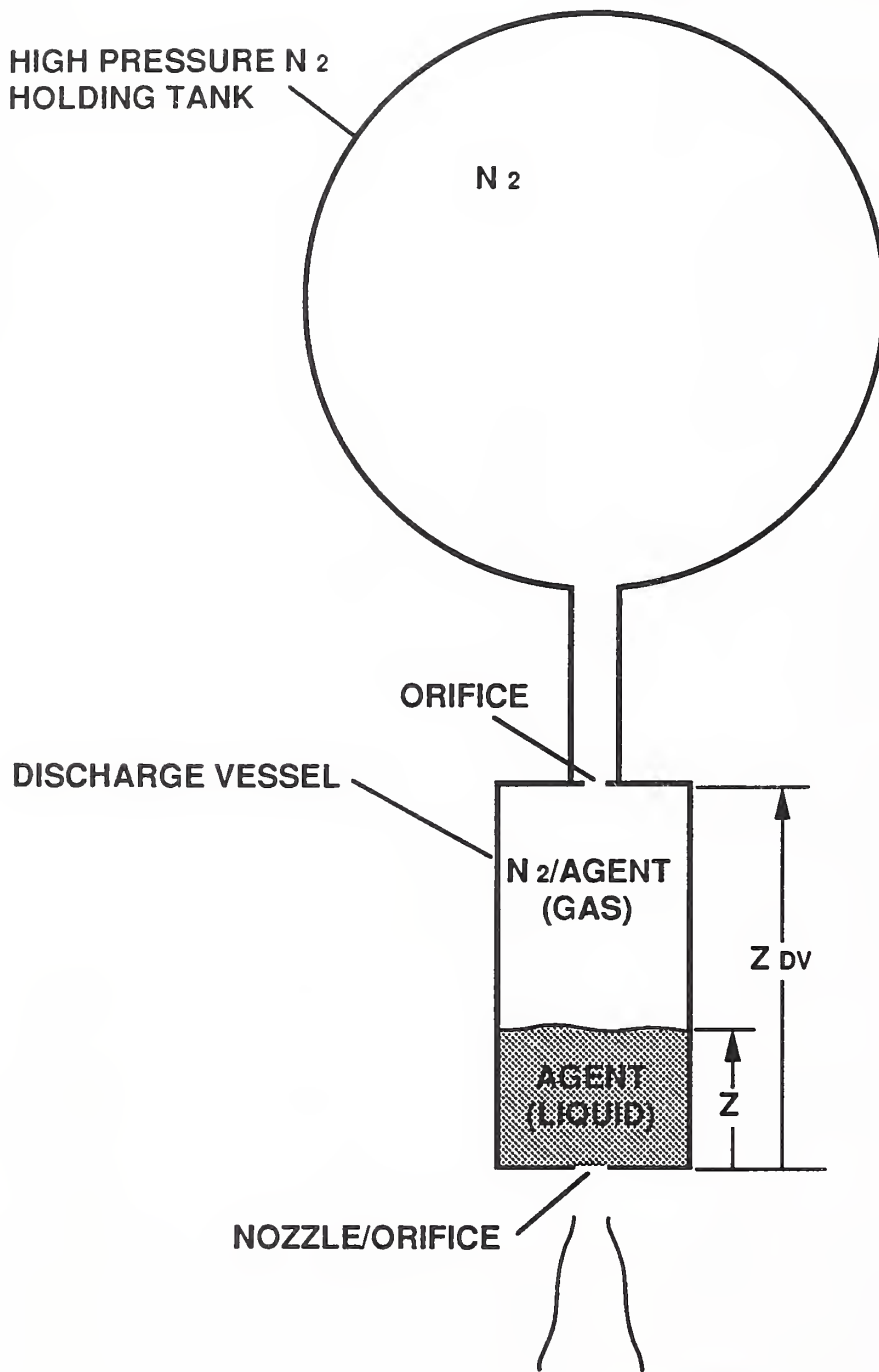


Figure 1. The experimental arrangement.

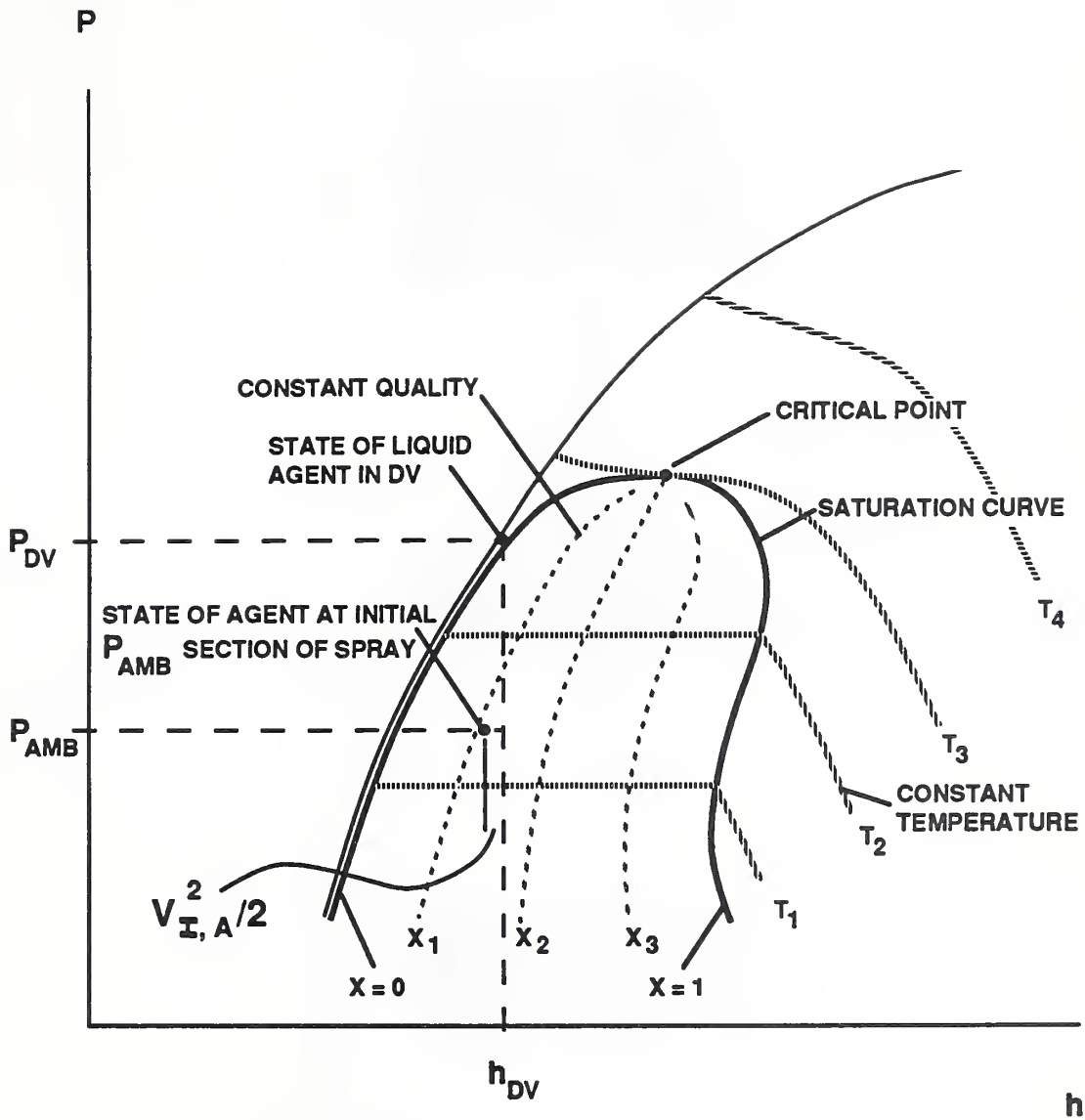


Figure 2. Path in the enthalpy - pressure plane of the thermodynamic state of the initially liquid agent as it flows from inside to outside the pressure vessel and achieves a stable two-phase state at the initial section.

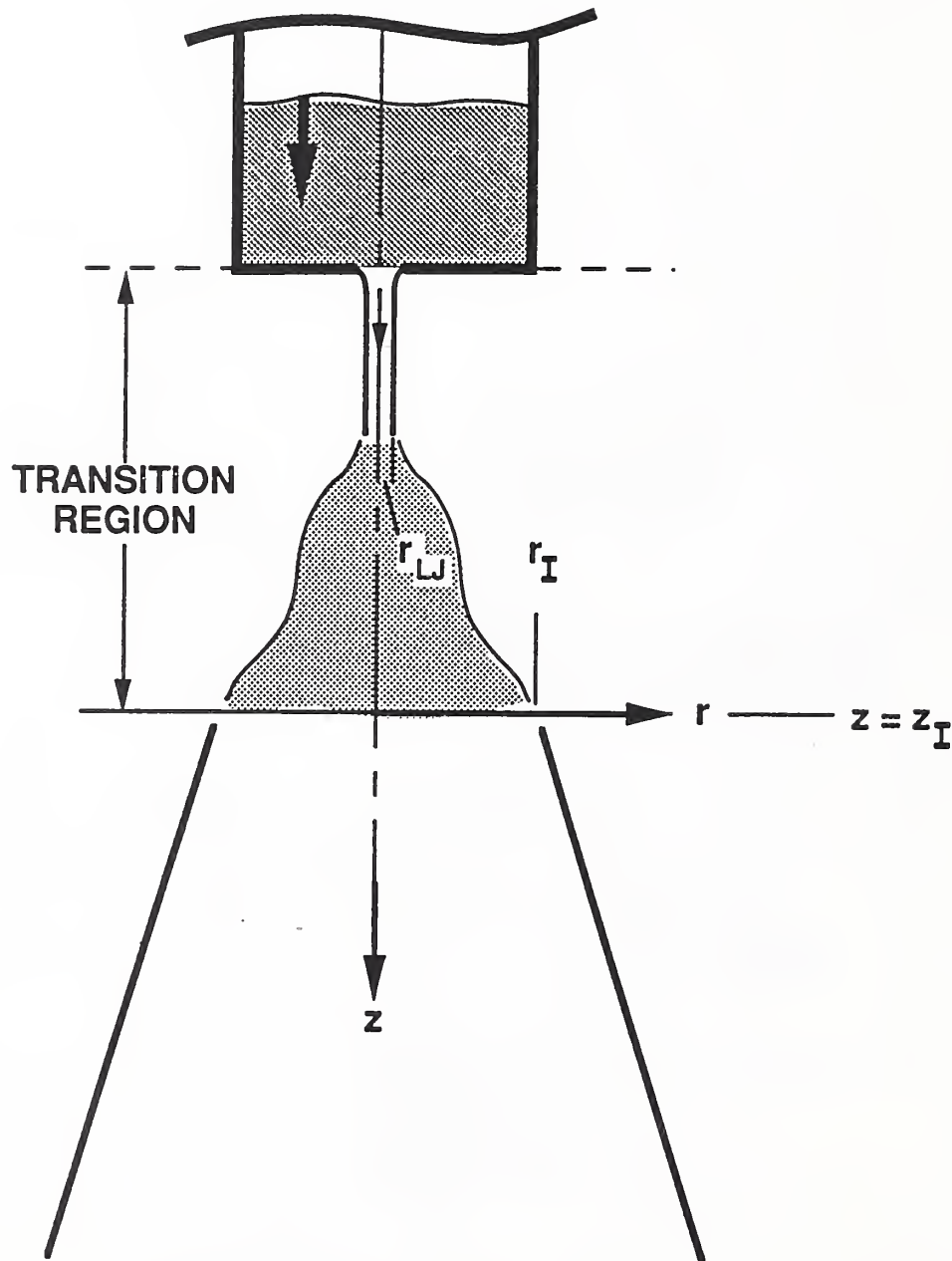


Figure 3. Sketch of the discharging agent, the transition region, and the initial section,  $z = z_I$ .

AT  $z = z_I$  :

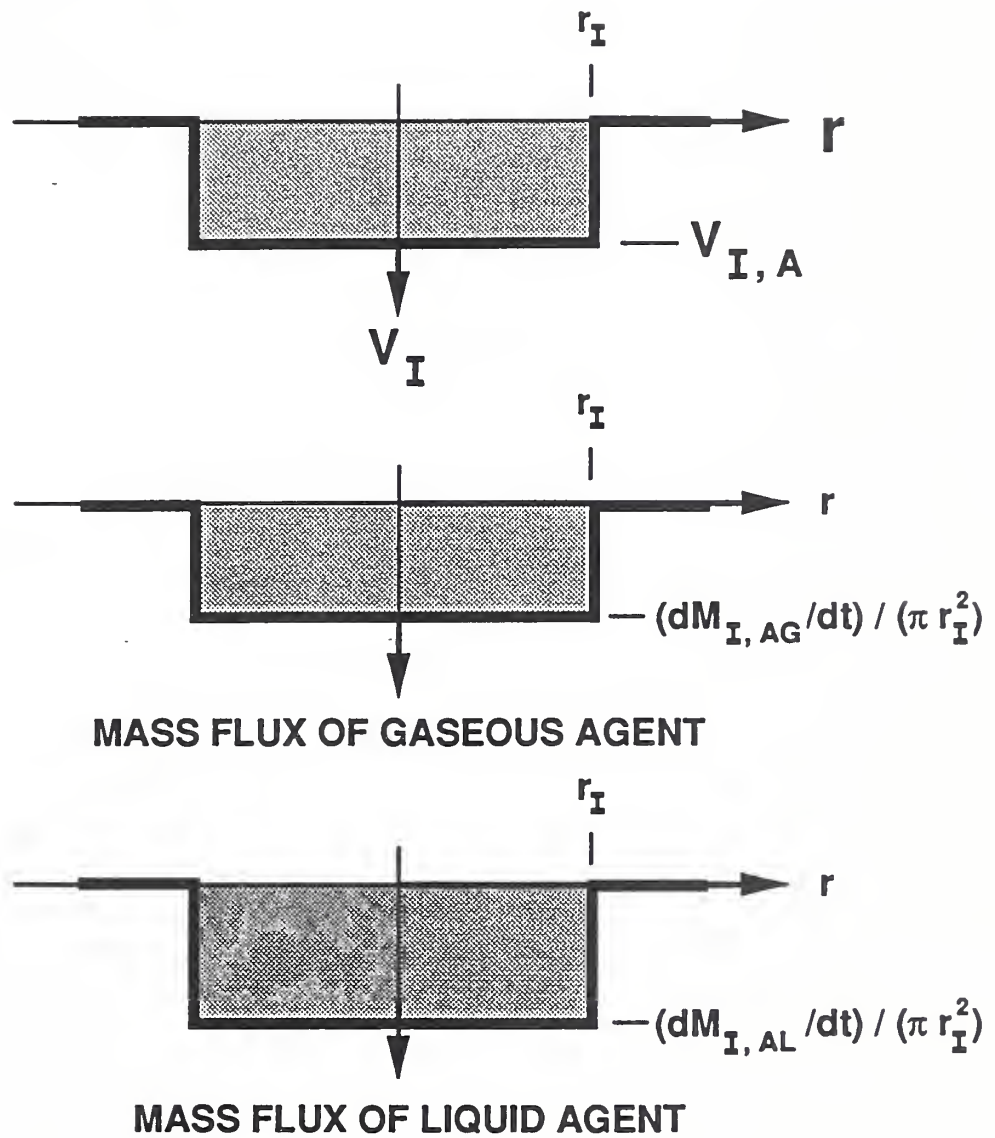


Figure 4. Sketch of the velocity and mass fluxes of agent gas and agent liquid droplets at the initial section,  $z = z_I$ .

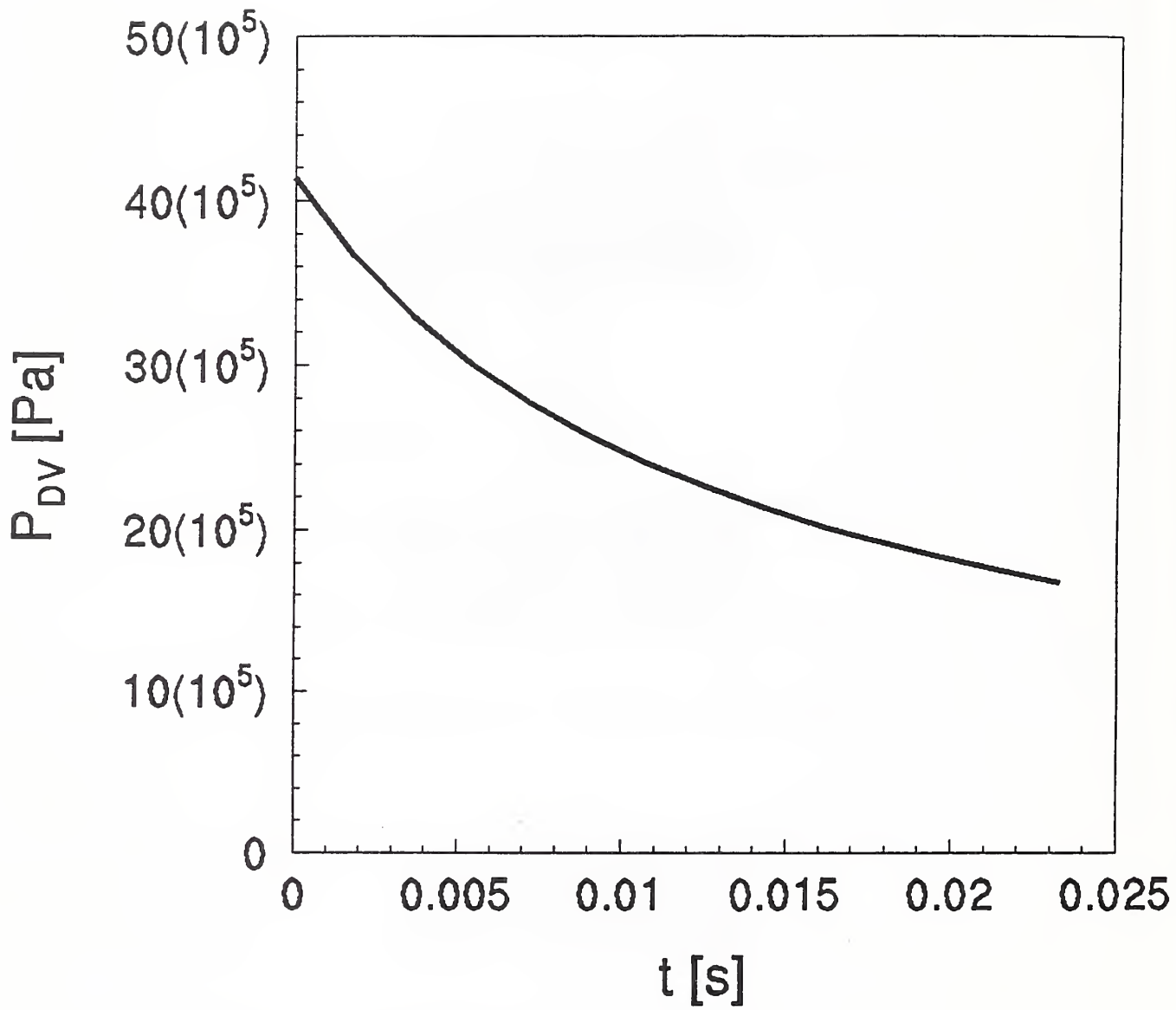


Figure 5. Plot of Table 3 results for  $P_{DV}$  as a function of time during vessel discharge of Freon 22.

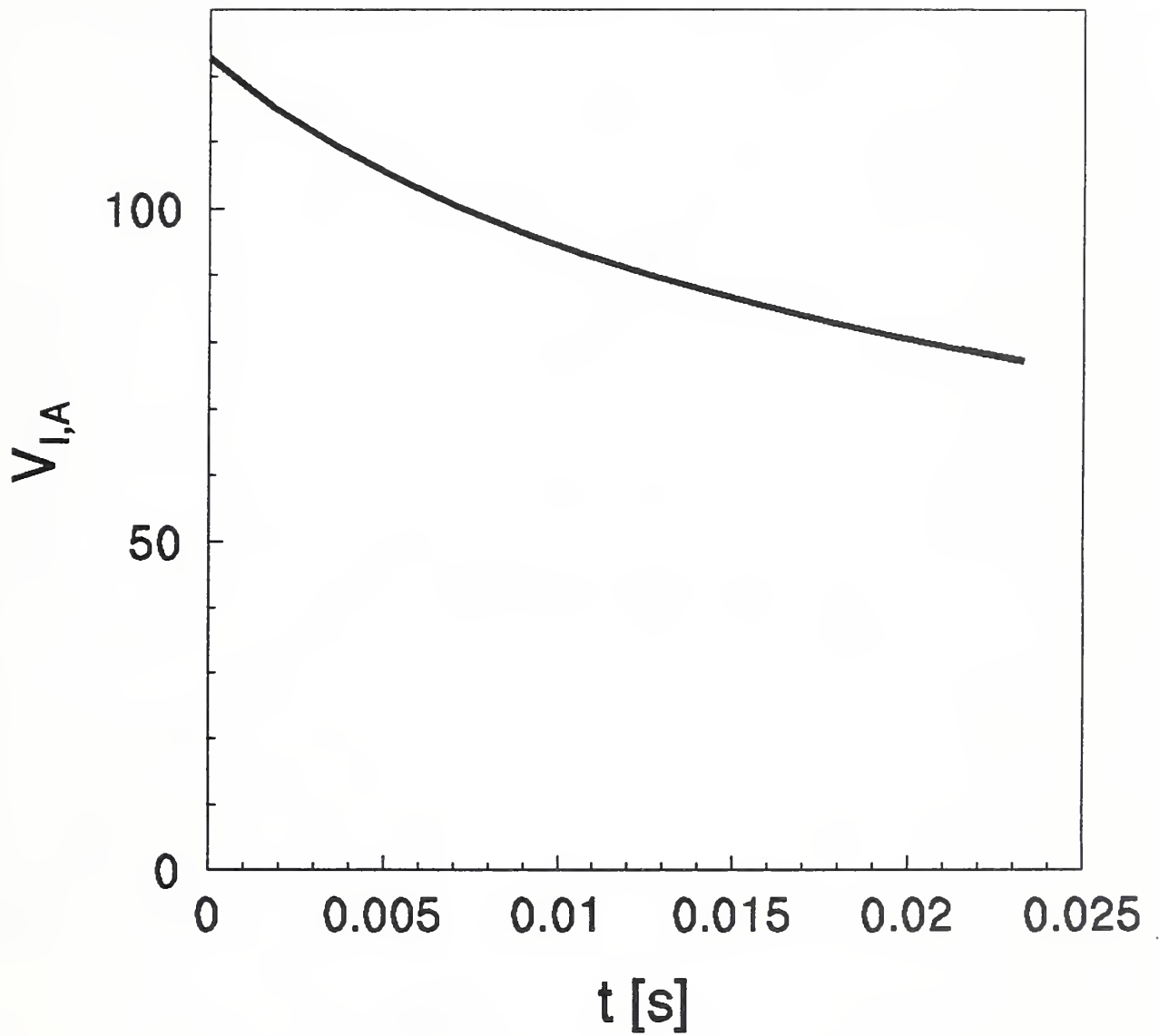


Figure 6. Plot of Table 3 results for  $V_{I,A}$  as a function of time during vessel discharge of Freon 22.

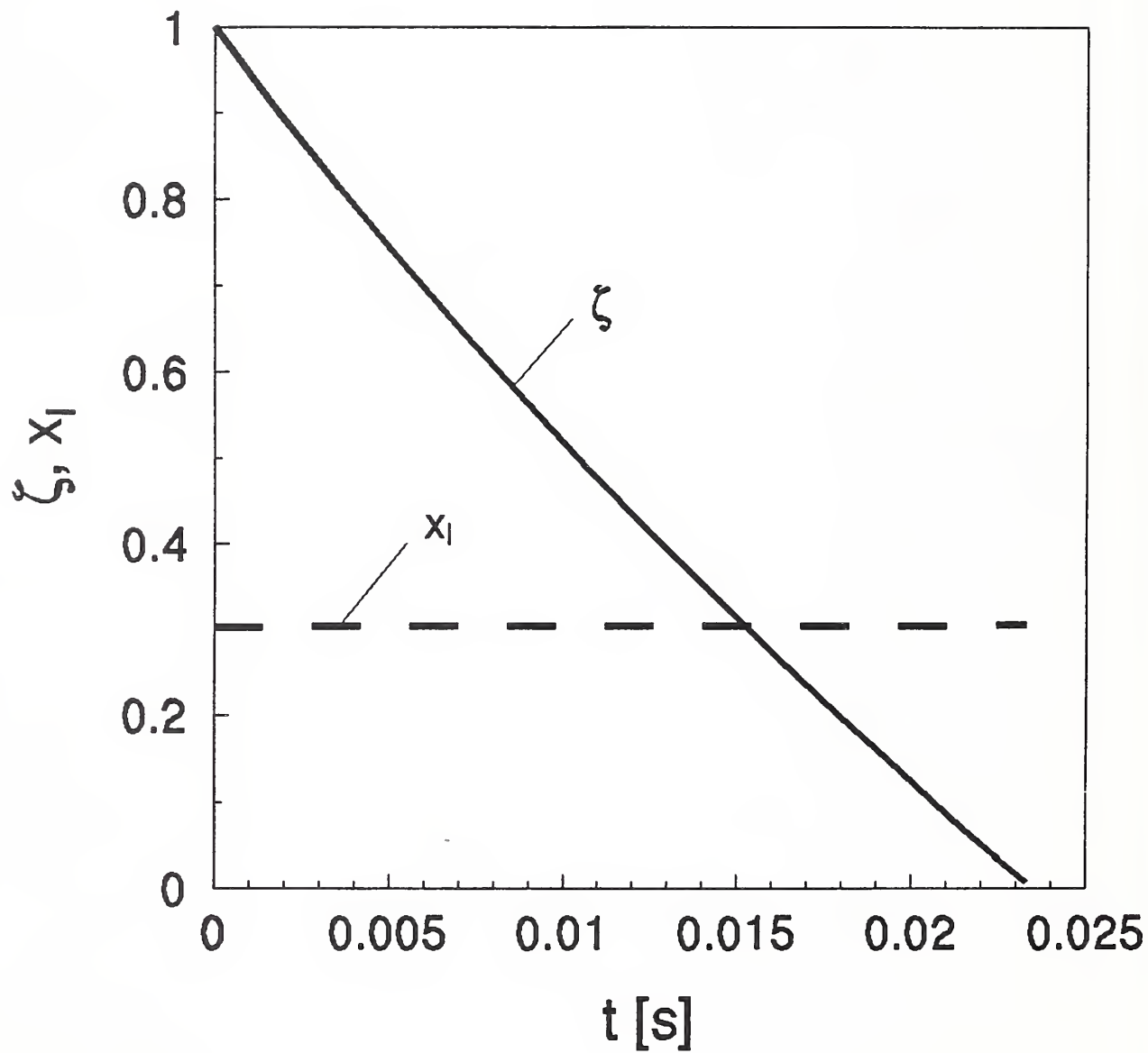


Figure 7. Plots of Table 3 results for  $\zeta$  and  $x_1$  as functions of time during vessel discharge of Freon 22.

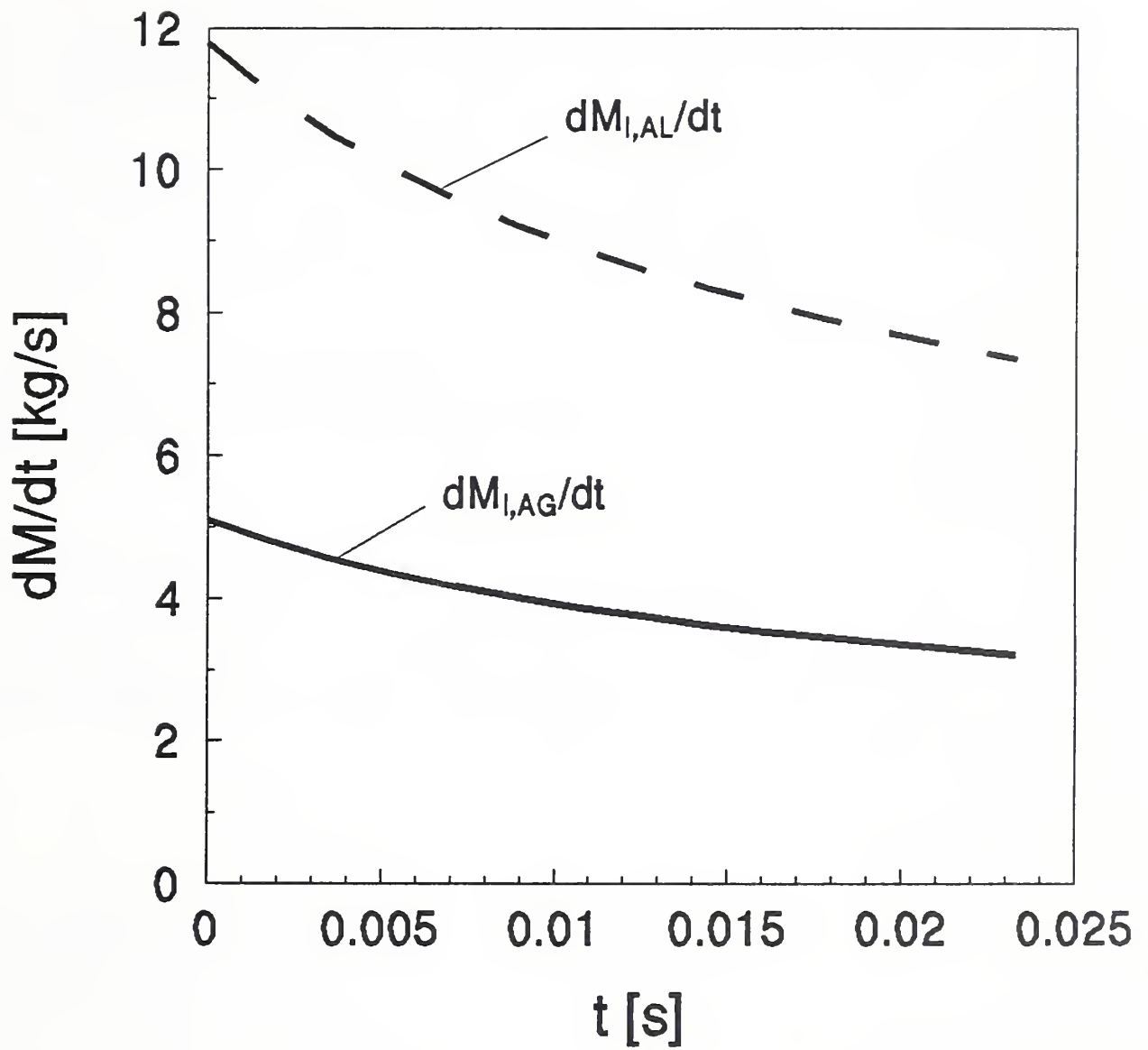


Figure 8. Plots of Table 3 results for  $dM_{I,AL}/dt$  and  $dM_{I,AG}/dt$  as functions of time during vessel discharge of Freon 22.



NIST-114  
(REV. 9-82)  
ADMAN 4.09

U.S. DEPARTMENT OF COMMERCE  
NATIONAL INSTITUTE OF STANDARDS AND TECHNOLOGY

(ERB USE ONLY)

ERB CONTROL NUMBER	DIVISION
PUBLICATION REPORT NUMBER NISTIR 5219	CATEGORY CODE
PUBLICATION DATE September 1993	NUMBER PRINTED PAGES

### MANUSCRIPT REVIEW AND APPROVAL

INSTRUCTIONS: ATTACH ORIGINAL OF THIS FORM TO ONE (1) COPY OF MANUSCRIPT AND SEND TO:  
THE SECRETARY, APPROPRIATE EDITORIAL REVIEW BOARD.

TITLE AND SUBTITLE (CITE IN FULL)  
The Dispersion of Fire Suppression Agents Discharged From High Pressure Vessels: Establishing Initial/Boundary Conditions for the Flow Outside the Vessel

CONTRACT OR GRANT NUMBER \_\_\_\_\_ TYPE OF REPORT AND/OR PERIOD COVERED \_\_\_\_\_

AUTHOR(S) (LAST NAME, FIRST INITIAL, SECOND INITIAL)  
Cooper, Leonard Y.

PERFORMING ORGANIZATION (CHECK (X) ONE BOX)  
 NIST/GAITHERSBURG  
 NIST/BOULDER  
 JILA/BOULDER

LABORATORY AND DIVISION NAMES (FIRST NIST AUTHOR ONLY)  
BFRL, Fire Safety Engineering Division

SPONSORING ORGANIZATION NAME AND COMPLETE ADDRESS (STREET, CITY, STATE, ZIP)  
US Air Force  
Wright Patterson AFB 45433-6563

RECOMMENDED FOR NIST PUBLICATION

<input type="checkbox"/> JOURNAL OF RESEARCH (NIST JRES)	<input type="checkbox"/> MONOGRAPH (NIST MN)	<input type="checkbox"/> LETTER CIRCULAR
<input type="checkbox"/> J. PHYS. & CHEM. REF. DATA (JPCRD)	<input type="checkbox"/> NATL. STD. REF. DATA SERIES (NIST NSRDS)	<input type="checkbox"/> BUILDING SCIENCE SERIES
<input type="checkbox"/> HANDBOOK (NIST HB)	<input type="checkbox"/> FEDERAL INF. PROCESS. STDS. (NIST FIPS)	<input type="checkbox"/> PRODUCT STANDARDS
<input type="checkbox"/> SPECIAL PUBLICATION (NIST SP)	<input type="checkbox"/> LIST OF PUBLICATIONS (NIST LP)	<input type="checkbox"/> OTHER _____
<input type="checkbox"/> TECHNICAL NOTE (NIST TN)	<input checked="" type="checkbox"/> NIST INTERAGENCY/INTERNAL REPORT (NISTIR)	

RECOMMENDED FOR NON-NIST PUBLICATION (CITE FULLY)  U.S.  FOREIGN

PUBLISHING MEDIUM  
 PAPER  CD-ROM  
 DISKETTE (SPECIFY) \_\_\_\_\_  
 OTHER (SPECIFY) \_\_\_\_\_

SUPPLEMENTARY NOTES

ABSTRACT (A 1500-CHARACTER OR LESS FACTUAL SUMMARY OF MOST SIGNIFICANT INFORMATION. IF DOCUMENT INCLUDES A SIGNIFICANT BIBLIOGRAPHY OR LITERATURE SURVEY, CITE IT HERE. SPELL OUT ACRONYMS ON FIRST REFERENCE.) (CONTINUE ON SEPARATE PAGE, IF NECESSARY.)

This work reports on part of an effort to study the dispersion and extinguishment effectiveness of Halon and Halon-alternative fire extinguishment agents discharged from  $N_2$ -pressurized vessels. In the systems under consideration, as the agent exits from the vessel, thermodynamic and fluid-dynamic instabilities lead to flashing and break-up of the agent into a two-phase droplet/gaseous jet mixture. This occurs in a transition region relatively close to the vessel exit orifice/nozzle. Downstream of this region the two-phase agent jet then mixes with the ambient air environment and is dispersed in the protected space.

A mathematical model has been developed previously to simulate the time-dependent discharge of the agent from the pressure vessel. Using the output of this model and thermodynamic and fluid-dynamic considerations of the phenomena in the transition section, the present work develops a method for determining a set of initial/boundary conditions at an initial section of the jet, downstream of the transition region. These initial/boundary conditions are in a form that can be used to formulate and solve the problem of the development and dispersal of the ensuing mixed air/two-phase-agent jet.

Example applications of the developed methodology are presented. These are for agent discharge from a half-liter cylindrical discharge vessel with a circular discharge nozzle/orifice of diameter 0.019m. Simulations involve discharge of the vessel when it is half-filled with either Freon 22 or Halon 1301 and then pressurized with  $N_2$  to  $41.37 \times 10^5$  Pa (600psi).

KEY WORDS (MAXIMUM 9 KEY WORDS; 28 CHARACTERS AND SPACES EACH; ALPHABETICAL ORDER; CAPITALIZE ONLY PROPER NAMES)

agents, aircraft fire safety, discharge, fire extinguishment, fire safety, halon, halon alternatives

AVAILABILITY

<input checked="" type="checkbox"/> UNLIMITED	<input type="checkbox"/> FOR OFFICIAL DISTRIBUTION. DO NOT RELEASE TO NTIS.
<input type="checkbox"/> ORDER FROM SUPERINTENDENT OF DOCUMENTS, U.S. GPO, WASHINGTON, D.C. 20402	
<input checked="" type="checkbox"/> ORDER FROM NTIS, SPRINGFIELD, VA 22161	

NOTE TO AUTHOR(S) IF YOU DO NOT WISH THIS MANUSCRIPT ANNOUNCED BEFORE PUBLICATION, PLEASE CHECK HERE.





